COMPARISON OF UV IRRADIANCE DATA FROM OMI WITH GROUND-BASED OBSERVATIONS AT THE CHISINAU (KISHINEV) SITE, MOLDOVA

A. Aculinin and V. Smicov

Institute of Applied Physics, Academy of Sciences of Moldova, Academiei str. 5, Chisinau, MD-2028 Republic of Moldova; e-mail: akulinin@phys.asm.md

(Received 5 October 2012)

Abstract

Erythemal UV irradiance data obtained from ground-based observations are used for validation of the UV products from overpass nadir measurements performed with the Ozone Monitoring Instrument (OMI) on-board the EOS Aura satellite platform. UV ground data were obtained with using of broadband radiometers (model UV-S-B-C) at the ground-based solar radiation monitoring station in Kishinev (Chisinau), Moldova during the period from 2004 to 2009. OMI UV final products were derived by the OMI's international team with using of the TOMS-like algorithm. Erythemal dose rate at time of overpass (OEDR) and at local noon time (EDR@noon) and erythemal daily dose (EDD) were taken into analysis. Interval of 1-min averaging of erythemal UV irradiance measurements with ground-based broadband radiometer gives an possibility to make quasi-synchronous observations with OMI overpass measurements. Validation showed that OMI overpass UV data underestimate UV data from ground observations for all sky (AS) and cloud-free (CF) conditions. Results of validation showed a bias value of –15.8% under AS and –18.3% under CF conditions. Concerning EDR@noon data bias was –15.8% under AS and –17.7% under CF conditions; taking into account EDD data some increasing in bias was observed (with a value of –21.5% and –19.9% under AS and CF conditions, respectively). The effect of aerosols on UV irradiance was studied in terms of aerosol optical depth (AOD@340 nm) retrieved from the AERONET, NASA/GSFC. It was observed that there is a high correlation of ~0.79 and that a larger relative difference corresponds to a larger value of AOD@340 nm.

1. Introduction

The study of variability of the UV radiation levels at the Earth's surface has been of intense interest in the last decades; the key issues were discussed and summarized in report [1]. This interest is due to issues concerning the well-known problem of ozone depletion [2]. The solar UV radiation passing through the atmosphere has a significant impact on human life, flora and fauna, and terrestrial and aquatic ecosystems. This impact may have both a positive and negative effect. For example, a negative effect is that high exposure to UV radiation is fraught with high risk of skin cancers, eye diseases (cataracts), and suppression of human immune system. In addition, UV radiation is involved into the complex chemical reactions with the vehicles exhausts resulting to the formation of smog, which is responsible for eyes and respiratory diseases.

Atmospheric ozone absorption, cloudiness, and aerosols are the main factors that affect UV radiation along the path from the top of the atmosphere to the Earth's surface. It should be noted that these factors demonstrate significant variability on spatial and time scales. To investigate UV irradiance variability on the spatial and temporal scales, both ground-based networks of spectral and broadband photometers and some satellite platforms with unique optical spectral instruments

are used. Ground-based or direct observations can be fulfilled at the small confined areas of Earth's surface. It is a great limitation. At the same time, satellite observations provide daily mapping with a global coverage from a single instrument on-board. The most known among the satellite instruments are the Total Ozone Mapping Spectrometer (TOMS)-like on-board the Earth Probe platform and the Ozone Monitoring Instrument (OMI) on-board the NASA EOS AURA platform. OMI instrument [3, 4] is the successor to the TOMS instruments and is in operation since September 2004.

Reliability of satellite UV irradiance data depends upon the accuracy of measurement by using of the unique spectral optical instruments aboard the satellite, models of atmosphere and atmospheric composition, which are applied in computer modeling and retrieving algorithms for data processing. In addition to instrumental errors, which affect the satellite UV measurements, there are modeling uncertainties in retrieving UV irradiance at the Earth's surface from backscattered UR radiation measured on the satellite orbit. In this connection, validation of satellite data through the ground-based direct UV observations is an extremely important condition of improving the quality and accuracy of UV irradiance data retrieved from satellites. The first thorough validation of the OMI UV products relative to the ground-based UV measurements can be found elsewhere [4]. Results of the study showed a good agreement with the ground spectral UV measurements. Results of validation OMI UV data versus the ground UV observations obtained at a number of stations in Europe can be found elsewhere [5-12]. In most cases, the comparison of OMI UV data with the ground-based UV data showed a good compliance, but having positive biases with values of a variable range for different locations.

Within the framework of this paper, we fulfilled validation of the UV irradiance data retrieved from OMI overpass measurements at the Aura satellite platform with the UV data obtained from direct observations at the ground-based station in the Institute of Applied Physics (IAP), Kishinev (Chisinau), Republic of Moldova in the course of period from 2004 to 2009. Ground-based erythemal UV data from a broadband radiometer were used in validation. Validation of OMI UV data through ground-based measurements will be fulfilled for erythemal UV irradiances or dose rates measured at the time of OMI overpass and at local noon time, and also for erythemal UV daily dose. Uncertainties in validation between OMI and ground-based data due to cloudiness and aerosol variability will be examined.

2. Measurement approach

Erythemal UV data retrieved from measurements of spectral components of solar radiation reflected or backscattered from the Earth's surface or from the top of clouds by using an OMI instrument [4] are utilized in this analysis. OMI is a nadir viewing ultraviolet/visible solar backscatter spectrometer in a wavelength range of 270 to 500 nm, and it is placed on-board the Aura satellite platform. UV irradiance data were retrieved from satellite spectral images of the Earth's surface with high spectral and spatial resolution. The small pixel size of the image corresponds to a dimension of 13 x 24 km^2 (for nadir viewing) of the area projected onto the Earth's surface. The instrument has a 2600 km wide viewing perpendicular to the line of flight of the space-borne AURA satellite platform. A more detailed description of the OMI instrument, some procedures of data processing, QC/QA procedures, calibration and characterization can be find elsewhere [3, 4]. Theoretical basis of the OMI algorithm for deriving the UV irradiance from spectral radiances scattered and reflected from the Earth's surface reposes on the TOMS-like algorithm (ver.8 is the last version) applied to OMI data processing, and it is described in detail elsewhere [13-16].

UV irradiance datasets retrieved from OMI overpass measurements are compared with the data from ground observations carried out with the UV broadband solar radiometers at the ground-based solar radiation monitoring station in the IAP. Ground observations of UV irradiance are being continuously carried out by the Atmospheric Research Group (ARG), IAP. Global and diffuse UV irradiances are measured with two broadband UV radiometers UV-S-B (Kipp&Zonen) installed at the radiometric complex. The complex is a key element of the ground-based solar radiation monitoring station at the Institute [17]. The station is situated in an urban environment of Kishinev (Moldova) and mounted at the Institute's building roof. Time-series of UV radiance at the ground station (φ=47.00^{0}N, λ_o=28.82^{0}E, h=205 m a.s.l.) started in September 2003. In addition, diffuse, direct, and global broadband solar radiation (280–3000 nm), global and diffuse UV-B (280–315 nm), global UV-A (315–400 nm) and PAR (400–700 nm) radiation, atmospheric IR radiation (4–42 μm), total column ozone content X, DU, and main surface meteorological parameters are measured at the ARG ground station [17]. Aerosol optical characteristics in a column of the atmosphere have been measured by using a Cimel-318 sunphotometer within the framework of the AERONET project, NASA/GSFC [18] since 1999. Datasets of daily means of aerosol optical characteristics are used for evaluation of aerosol effect upon the validation results. UV irradiance data collected over the period of OMI satellite and ARG ground-based observations from 2004 to 2009 are used in this analysis.

3. Data analysis

Respective UV irradiance data from direct ground observations were processed and compiled into the arrays of data; hereinafter, these datasets will be referred to as ARG. Multi-year series of UV data retrieved from the OMI measurements at the Aura satellite platform since October 2004 are utilized in validation. OMI UV final products are available at the Aura Validation Data Center (AVDC) web-site [19].

Summary of statistics concerning the validation of the OMI UV irradiance data in comparison with the ARG ground observations are presented in Table 1. The following parameters are taken in account: *n* is the number of days representing pairs of ARG and OMI data of synchronous observations taken into account in comparison; *R* is the correlation coefficient between ARG ground and OMI data; the slope of regression line of the scatterplot; *b* (in %) is the mean relative difference or bias defined as $b = \frac{1}{n}\sum_{i=1}^{n}(\frac{y_i - x_i}{x_i})\cdot 100$; the root mean squares (RMS) expressed in mW·m^{-2} or J·m^{-2}, and in % were computed as follows: $\sqrt{\frac{1}{n}\sum_{i=1}^{n}(y_i - x_i)^2}$ and $\sqrt{\frac{1}{n}\sum_{i=1}^{n}(\frac{y_i - x_i}{x_i})^2}\cdot 100$, respectively.

Variables y_i and x_i represent the pairs of data from the OMI overpass (y_i) and ARG ground (x_i) observations of UV irradiance. OMI UV products include erythemal dose rate at time of overpass (OEDR) and at local noon time (EDR@noon), and erythemal daily dose (EDD). These datasets for coordinates (φ,λ_o) of the ARG ground station were retrieved from the AVDC database [19]. The ARG UV data consist of 1-min averaged measurements of erythemal UV irradiance by using of UV-S-B-C broadband radiometers. These datasets were processed taking into account the respective lookup tables (X,θ) with a matrix of adjustment factors computed for the set of values of total ozone content X and solar zenith angles θ. The EDRs and EDD data were obtained by weighting UV irradiance with the standard erythemal action spectrum CIE-1987 [20] and by

integration over the spectral wavelength range of 280–400 nm.

The ARG datasets were collected at the ground station for the period from October 2004 to November 2009 and consist of some parameters, such as instantaneous (OEDR and EDR@noon) and daily doses or daily totals (EDD) of erythemal UV irradiance measured both under all sky (AS) and cloud-free (CF) conditions. The scatter plots and time series presented below consist of data from the OMI overpass measurements versus to the ARG ground-based direct UV irradiance measurements. To keep the condition of spatial homogeneity of ARG and OMI data for validation, we introduce the following criterion of spatial restriction: pairs of ARG and OMI UV data will be taken into consideration only if the normal from a point with coordinates of the ARG ground station to the OMI tracking line is r< 24 km; hereinafter, the measurements will be referred to as point ones. At the same time, it was clearly pointed in [8, 10] that validation results should be considered with caution because of using the different spatial scales: ground-based measurements are fulfilled at a fixed point, whereas the satellite measurements have the spatial resolution of one pixel, which covers different areas from nadir viewing to the edges of swath viewing. Within these areas, UV measurements are affected by cloud and aerosol variability. Meanwhile, the sky condition factor, namely cloudiness variability, remains to be the main source of uncertainties and disagreements in validation of OEDR, EDR@noon, and EDD. This was due to the fact that sky conditions or cloud variability at the time of OMI overpass, as a rule, differ from those at the time of local noon or in the course of all day at which OEDR, EDR@noon, and EDD are measured and calculated. Time sampling with 1-min averaging applied for ground-based measurements of UV irradiance is sufficient to consider ARG ground and OMI overpass observations to be quasi-synchronous within the time window of ±1 min. To estimate the cloud variability onto validation, two cases were considered: all sky and cloud-free conditions. Optical cloud depth with $\tau_{cld} < 0.1$ and Lambertian Equivalent Reflectivity (LER) at $\lambda = 360$ nm with LER < 10% were used as criteria to select datasets corresponding to the cloud-free or cloudless conditions. Values τ_{cld} and LER are also presented in datasets retrieved from AVDC database [19] for coordinates (φ, λ_o) corresponding to the ARG ground-based station.

In addition, aerosol variability affects UV irradiance both in time and spatial scales in the same way as for the cloudiness mentioned above. At time of overpass, this characteristic differs from the analogous ones taking place at other time scales, such as local noon time and over the period of a day used in a computer modeling of OMI UV irradiances. It should be mentioned that the effect of aerosol variability is also observed within the satellite pixel area as was noted in [8, 10, 12]. Aerosol optical characteristics, such as aerosol optical depth (AOD) $\tau_a(\lambda)$ and retrieved aerosol single scattering albedo (SSA) from the AERONET observations [18] at the Kishinev site, are used in analysis and evaluation of aerosol effect on uncertainties of validation of OMI data through the ARG ground observations. Cloud and aerosol variability on various time scales, such as at overpass time, at local noon time, and over diurnal interval, are the main sources of uncertainties in validation of OMI UV data with those ones measured at the ground stations.

Scatterplots of the OEDR, EDR@noon, and EDD data derived from direct ARG ground-based observations at the Kishinev site and retrieved from OMI overpass measurements are shown in Figs. 1-3. Equations of regression lines are presented by a solid line in each of the figures. For each of the parameters, i.e., OEDR, EDR@noon, and EDD, the scatterplots are grouped separately by pairs, representing measurements carried out under AS (left side) and CF (right side) conditions, respectively. It is of particular interest to study the OEDR data, because the ARG ground-based observations are quasi-synchronous relative to the OMI overpass measurements, since the time difference is no more than ±1 min. Comparison between ARG observations and OMI modeled data for parameters EDR@noon and EDD will be burdened with

errors due to the uncertainty of cloudiness and aerosol variability over large time scales apart from overpass. Selection of the case with the CF condition gives the possibility to eliminate the cloudiness uncertainties and to estimate the effect of the aerosols through their optical characteristics.

It should be emphasized that the scatterplots reveal a high correlation between the OMI and ARG UV data both for AS and CF conditions. The scatterplots for CF conditions show a strong mutual dependence between the OMI and ARG UV data with a correlation coefficient of R =0.98. Under the AS condition, the correlation is slightly less than under the CF condition. For each of the parameters, the slopes of regression lines for the two types of sky conditions are different. In the case of the CF condition, the slopes of regression line are larger than the ones computed under the AS condition. At the same time, it should be noted that, for all parameters and sky conditions, the slopes of regression line are less than 1; that is, the OMI derived surface UV data underestimates ARG ground UV data. We note that mean relative differences or biases b are negative values for all parameters and sky conditions under examination. The values of biases are in a range of −15.8% to −21.5%. A comparison of the OMI and ARG OEDRs data at time of overpass taking into account the data under the CF condition shows a negative bias b of −18.3% with a correlation of R = 0.98 . For the AS condition, the bias and correlation are b = –15.8% and R = 0.93, respectively. Scatterplots for EDD and EDR@noon data from OMI and ARG observations are shown in Figs. 2 and 3, where (a) and (b) denote the AS and clear sky conditions, respectively. A summary of erythemal OMI UV validation results including the correlation coefficient, slopes, RMS (in %, mWm^{-2}, and Jm^{-2}), and biases (in %) is presented in the table.

Table. Summary of erythemal OMI UV validation results (n is the number of days of observations taken into account in the comparison; r is the correlation coefficient between ARG ground and OMI overpass data; RMS is the root mean squares; b (bias) is the mean relative difference. The data are presented for AS and CF conditions. The bias and RMS are computed for OMI overpass data relative to ARG data acquired from ground observations. Period of observation: October 2004 to November 2009)

		n	R	slope	RMS	b(bias), %
OEDR	(AS)	1144	0.93	0.79	34.8 $mW \cdot m^{-2}$ (44.4%)	–15.8
	(CF)	64	0.98	0.87	28.7 $mW \cdot m^{-2}$ (20.4%)	–18.3
EDD	(AS)	1144	0.97	0.83	783 $J \cdot m^{-2}$ (27.4%)	–21.5
	(CF)	64	0.98	0.85	788 $J \cdot m^{-2}$ (21.9%)	–19.9
EDR@noon	(AS)	1144	0.93	0.79	44.4 $mW \cdot m^{-2}$ (34.8%)	–15.8
	(CF)	64	0.98	0.87	31.5 $mW \cdot m^{-2}$ (20.0%)	–17.7

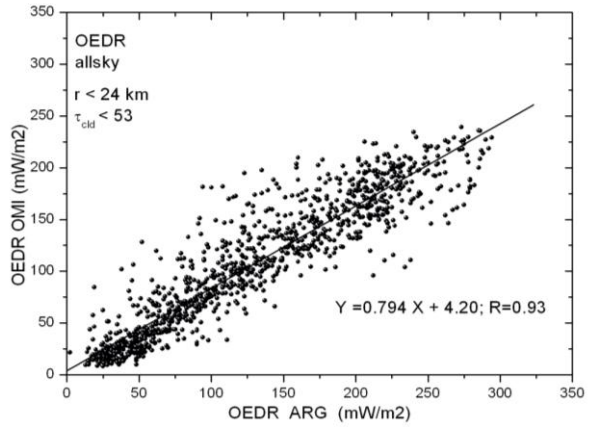

Fig. 1a. Comparison of the OEDR (in $mW \cdot m^{-2}$) from the ARG radiometer and from OMI at the time of overpass for AS conditions.

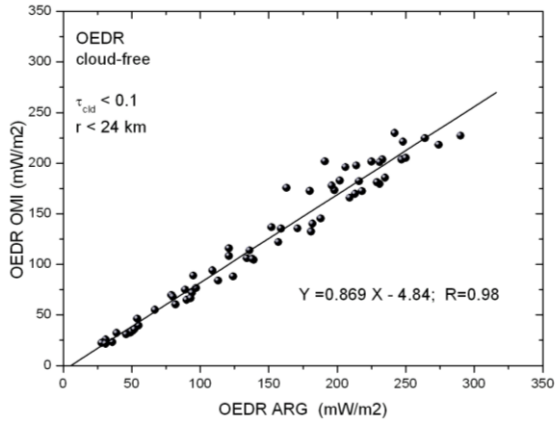

Fig. 1b. Comparison of the OEDR (in $mW \cdot m^{-2}$) from the ARG radiometer and from OMI at the time of overpass for CF conditions.

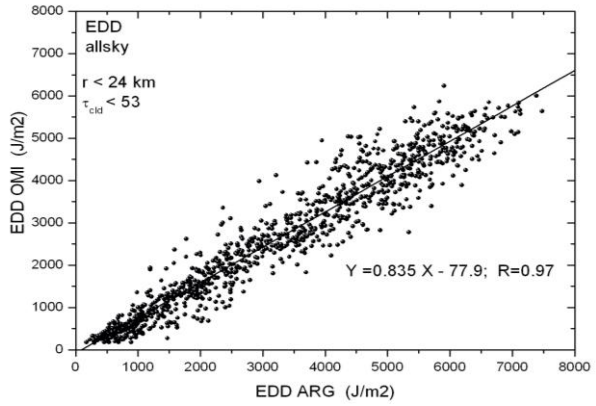

Fig. 2a. Comparison of the EDD (in $J \cdot m^{-2}$) from the ARG radiometer and from OMI for AS conditions.

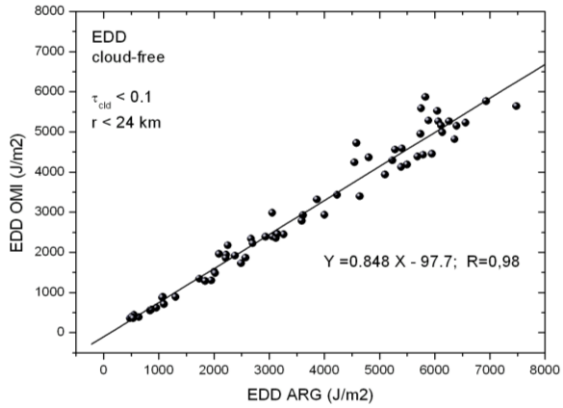

Fig. 2b. Comparison of the EDD (in $J \cdot m^{-2}$) from the ARG radiometer and from OMI for CF conditions.

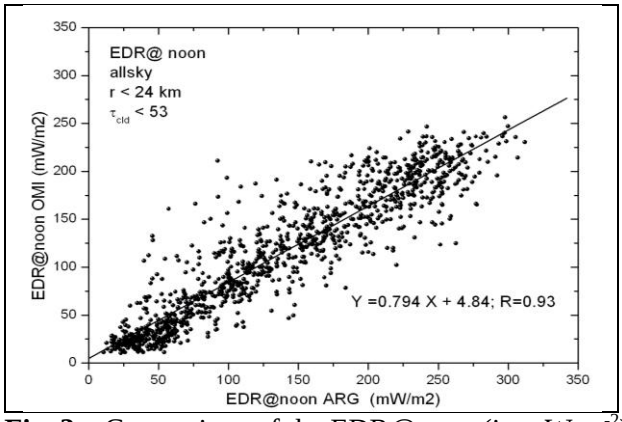

Fig. 3a. Comparison of the EDR@noon (in $mW \cdot m^{-2}$) from the ARG radiometer and from OMI for AS conditions.

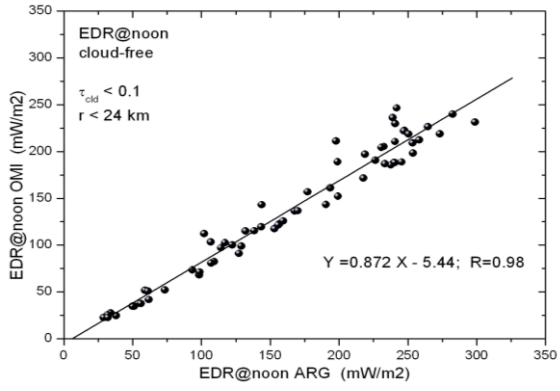

Fig. 3b. Comparison of the EDR@noon (in $mW \cdot m^{-2}$) from the ARG radiometer and from OMI for CF conditions.

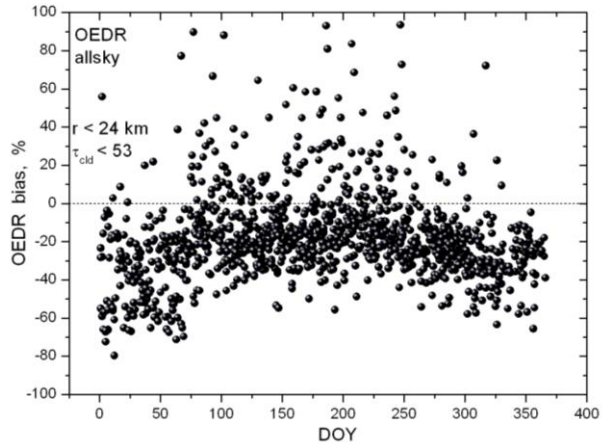

Fig. 4a. Time series of the relative differences or bias (in %) between the ARG ground-based and OMI OEDR for AS conditions.

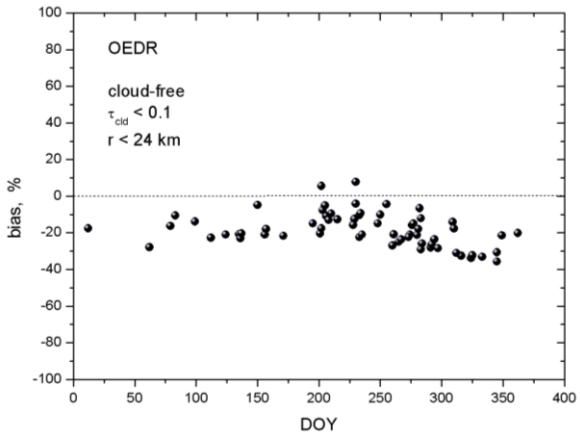

Fig. 4b. Time series of the relative differences or bias (in %) between the ARG ground-based and OMI OEDR for CF conditions.

Seasonal variation of relative differences *b* versus day of year (DOY) is shown in Fig. 4 for AS (a) and CF (b) conditions. Time series of biases *b* reveals a seasonal variability. The range of bias variation between winter and summer months is on an average ~26% and ~14% under AS and CF conditions, respectively. This can be indicative of a mismatch between the really existing surface albedo and aerosol models and the ones used in modeling. Meanwhile, the cloudiness remains an important factor resulting in large uncertainties in validation of OMI UV irradiance data through ARG ground-based UV data. A large dispersion in bias data due to cloudiness is observed for AS conditions (see Fig. 4a).

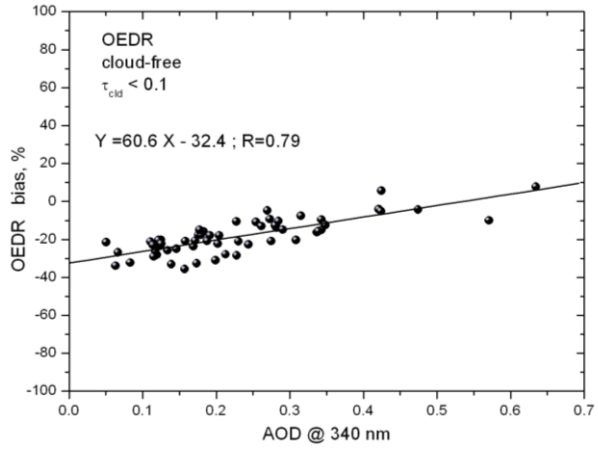

Fig. 5. Relative differences or bias (in %) between the ARG ground-based and OMI OEDR as a function of AOD at 340 nm for CF conditions.

Under CF conditions, the AOD was retrieved from the spectral measurements using the Cimel-318 sun photometer installed at the ground-based station in IAP, Kishinev (Moldova). Aerosol optical properties were measured and retrieved within the AERONET project. For evaluation, we used the data on AOD@340 nm measured at λ = 340 nm, which is the shortest wavelength in the UV spectral range of the sun photometer. To evaluate the effect of AOD on the relative differences *b*, the UV OEDR under CF conditions was chosen in order to exclude the effect of cloudiness and to use quasi-synchronous measurements at time of overpass. Figure 5 shows the existence of a correlation between relative differences *b* and AOD@340 nm with respective regression line indicated in the same figure. The larger relative difference *b* corresponds to the larger value of AOD, and the correlation between *b* and AOD is $R = 0.79$.

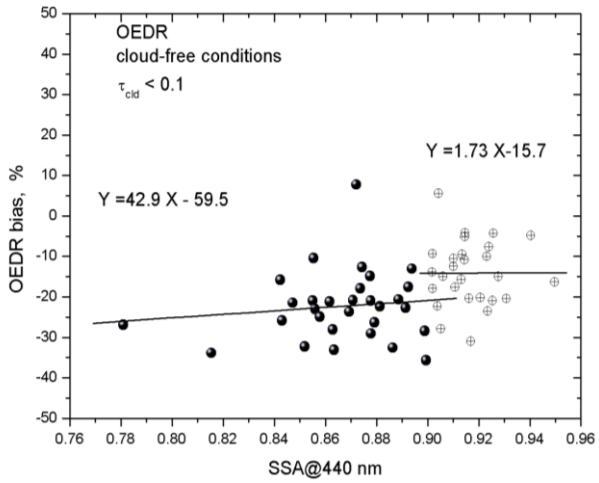

Fig. 6. Relative differences (in %) between the ARG ground-based and OMI OEDR as a function of SSA at 440 nm for CF sky conditions.

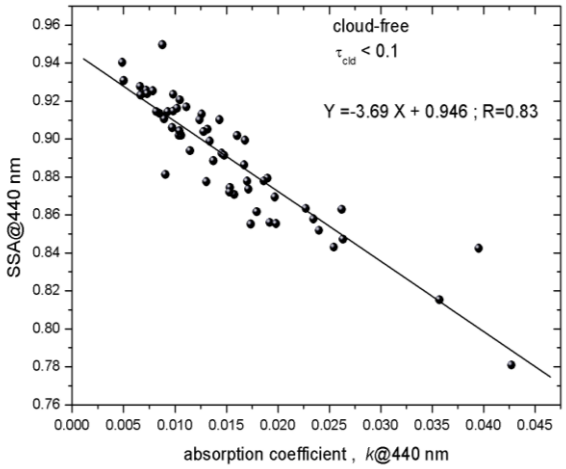

Fig. 7. Variation of SSA at 440 nm as a function of aerosol absorption coefficient *k* for CF sky conditions. The equation of regression line (solid line) is indicated.

Figure 6 shows the dependence between the relative differences *b* and aerosol SSA at λ = 440 nm (SSA@440 nm) with respective regression lines representing medium SSA < 0.9 and low SSA > 0.9 absorptive aerosols. Respective regression lines are indicated in the same figure. The relationship between SSA@440 nm and aerosol absorption coefficient *k* at λ = 440 nm is shown in Fig. 7. Figure 7 clearly shows that the aerosol SSA decreases with increasing aerosol absorption coefficient *k.* The correlation coefficient between SSA@440 and *k* is *R* = 0.83. Aerosol SSA@440 nm and *k* at λ=440 nm were retrieved from direct sun and diffuse sky spectral observations with a Cimel-318 sun photometer. The period of observation is October 2004 to November 2009. The dependences shown in Figs. 6 and 7 are derived for CF conditions.

4. Summary and conclusions

The aim of this study was to compare the OMI UV data with the measurements performed by using broadband UV radiometers at the ground-based based solar radiation monitoring station ARG IAP Kishinev (Moldova) for the period of observation from 2004 to 2009. Validation results were summarized in the table in terms of relative differences or biases *b*, correlation coefficients *R*, equation of regression lines, and RMS. OEDR, EDR@noon, and EDD parameters were considered in validation. Datasets were subdivided into two main groups of measurements carried out under AS and CF conditions. UV data were complemented with aerosol optical properties, such as AOD, aerosol SSA, and aerosol absorption coefficient *k*. These characteristics were retrieved from spectral measurements by using a Cimel-318 sun photometer operating at the solar radiation monitoring station within the AERONET project.

Comparisons of the OMI and ARG ground-based UV datasets showed that, on average, OMI data underestimate ARG measurements by more than –16%. It should be noted that, in all cases, the comparison showed negative relative differences or biases *b* with a high correlation between OMI and ARG UV datasets with *R* > 0.93. The correlation under CF conditions is higher than under AS conditions, and it is *R* = 0.98. The comparison for OEDR data showed a bias value of –15.8% under AS and –18.3% under CF conditions. Concerning EDR@noon data, the bias

is –15.8% under AS and –17.7% under CF conditions; taking into account the EDD data, an increase in bias is observed (with a value of –21.5% and –19.9% under AS and CF conditions, respectively). Time series of biases *b* reveals a seasonal variability. The range of bias variation between winter and summer months is, on an average, ~26% and ~14% under AS and CF conditions, respectively.

It was observed that the correlation between relative differences for OEDR data and AOD@340 nm under CF conditions is $R = 0.79$. The larger relative difference *b* corresponds to the larger value of AOD@340 nm.

The OMI underestimation of the ARG UV data can be partly explained by uncertainties due to aerosol optical-microphysical and climatic surface albedo at 360 nm models, which were applied in modeling of the OMI surface UV radiation from orbital measurements of surface backscattered UV radiation. During the measurement campaign at time of overpass, these models can differ from those existing in reality in the area of observation in the vicinity of the ground-based station. In this connection, another source of uncertainties in validation consists in the fact that ground-based measurements are fulfilled at a single point, where the ground-based station is placed, whereas the satellite output product represents an average over a variable area of the OMI pixel projection onto the Earth's surface.

Acknowledgments. The authors are grateful to the OMI International Science Team from KNMI and from the NASA Aura Validation Data Center (AVDC) for providing OMI data for our ground station. Special thanks to Dr. B. Holben and to AERONET science team from NASA/GSFC for providing a Cimel CE-318 sunphotometer and for its calibration, and for analyzing the Cimel data.

References

[1] Bais A.F., D. Lubin, et al., Global Ozone: Past and Present, p.7.1-7.54; Chapter 7 in *Scientific Assessment of Ozone Depletion: 2006*, Global Ozone Research and Monitoring Project–Report No. 50, 572 pp., World Meteorological Organization, Geneva, Switzerland (2007).

[2] Chipperfield M. P., Fioletov V. E., et al., Global Ozone: Past and Present, p.3.1-3.58; Chapter 3 in *Scientific Assessment of Ozone Depletion: 2006,* Global Ozone Research and Monitoring Project–Report No. 50, 572 pp., World Meteorological Organization, Geneva, Switzerland (2007).

[3] OMI Algorithm Theoretical Basis Document(ATBD), vol.I, OMI Instrument, Level 0-1b processor, Calibration &Operations; Ed. by P.F. Levelt, ATBD-OMI-01, ver.1.1, 50pp., August 2002, http://www.knmi.nl/omi/documents/data/OMI_ATBD_Volume_1_V1d1.pdf .

[4] Levelt P.F., van den Oord G.H.J., Dobber M.R., Malkki A., Huib Visser, Johan de Vries Stammes P., Lundell J.O.V., and Saari H., *Geoscience and Remote Sensing, IEEE Transactions,* 44 (5), 1093 (2006).

[5] Tanskanen A., Lindfors A., Määttä A., Krotkov N., Herman J., Kaurola J., Koskela T., Lakkala K., Fioletov V., Bernhard G., McKenzie R., Kondo Y., O'Neill M., Slaper H., den Outer P., Bais A.F., and Tamminen J., *J. Geophys. Res.*, 112, D24S44, doi:10.1029/2007JD008830 (2007)

[6] Buchard V., Brogniez C., Auriol F., Bonnel B., Lenoble J., Tanskanen A., Bojkov B., and Veefkind P., *Atmos. Chem. Phys*, v. 8, 4517-4528 (2008).
[7] Ialongo I., Casale G. R., and Siani A. M., *Atmos. Chem. Phys*, v. 8, 3283-3289 (2008).
[8] Weihs P., Blumthaler M., Rieder H. E., Kreuter A., Simic S., Laube W., Schmalwieser A.W., Wagner J. E., and Tanskanen A., *Atmos. Chem. Phys.* 8, 5615 (2008).
[9] Kazadzis S., Bais A., Arola A., Krotkov N., Kouremeti N., and Meleti C., *Atmos. Chem. Phys*, 9, 585 (2009).
[10] Kazadzis S., Bais A. , Balis D., Kouremeti N., Zempila M., Arola A., Giannakaki E., Amiridis V., and Kazantzidis A., *Atmos. Chem. Phys.* 9, 4593 (2009).
[11] Antón M., Cachorro V. E., Vilaplana J. M., Toledano C., Krotkov N. A., Arola A., Serrano A., and de la Morena B., *Atmos. Chem. Phys.*, 10, 5979 (2010).
[12] Cachorro V., Toledano C., Anton M., Berjon A., de Frutos A., Vilaplana J., Arola A., and Krotkov N., *Atmos. Chem. Phys.* 10, 11867 (2010).
[13] Tanskanen A., Krotkov N.A., Herman J.R., and Arola A., *IEEE Trans. Geo. Rem. Sens*., 44 (5), 1267, doi:10.1109/TGRS.2005.862203 (2006).
[14] OMI Algorithm Theoretical Basis Document(ATBD) Vol. III OMI Clouds, Aerosols, and Surface UV Irradiance; Ed. by P. Stammes, NASA Goddard Space Flight Center, Greenbelt, Maryland, USA, ATBD-OMI-03, ver. 2.0, 114 pp., August 2002 http://www.knmi.nl/omi/documents/data/OMI_ATBD_Volume_3_V2.pdf
[15] Krotkov N. A., Barthia P. K., Herman J. R., Fioletov V., and Kerr J., *J. Geophys. Res*., 103, 8779 (1998).
[16] Krotkov N. A., Herman J. R., Barthia P. K., Fioletov V., and Ahmad Z., *J. Geophys. Res*., 106, 11743 (2001).
[17] Aculinin A., Smirnov A., Smicov V., Eck T., and Policarpov A., *Mold. J. Phys. Sci.*, 3 (2), 204 (2004).
[18] Holben B.N., Eck T.F., Slutsker I., Tanre D., Buis J.P., Setzer A., Vermote E., Reagan J.A., Kaufman Y., Nakajima T., Lavenu F., Jankowiak I., and Smirnov A., *Rem. Sens. Environ.* 66, 1 (1998).
[19] Aura Validation Data Center(AVDC), http://avdc.gsfc.nasa.gov/index.php?site=2045907950
[20] McKinlay A.F. and Diffey B.L.., A reference action spectrum for ultraviolet induced erythema in human skin. In *Human Exposure to Ultraviolet Radiation: Risks and Regulations*. W.F. Passchier and B.F.M. Bosnjakovich, eds., International Congress Series, 83-87 (1987).